ELSEVIER

Thin Solid Films 334 (1998) 65–70

thin solid films

Lateral force microscopy investigations of the crystallization of $SrBi_2Ta_2O_9$ thin films

Kwang Bae Lee[a,*], Byeung Kwon Ju[b]

[a] *Department of Physics, Sangji University, Wonju, Kangwondo 220-702, South Korea*
[b] *Electronic Materials and Devices Research Center, KIST, Seoul 130-650, South Korea*

Abstract

A lateral force microscope (LFM) was used for studying the surface morphologies of $SrBi_2Ta_2O_9$ thin films with varying post-annealing temperature. Specimens were prepared onto platinized silicon wafers by the sol–gel method and post-annealed at 600–800°C. Non-ferroelectric matrix phases were found for specimens annealed below 700°C, which were confirmed by the measurement of X-ray diffraction (XRD) patterns. The friction coefficients between the surface of ferroelectric grain and non-ferroelectric matrix, and the silicon nitride tip, were determined from the line profile of the LFM images. The measured coefficients of friction for a tip on grain and matrix are 0.19 ± 0.08 and 0.28 ± 0.08, respectively. In the LFM images, the matrix phases decreased with increasing post-anneal temperature and the surfaces of the specimens annealed above 700°C were filled with SBT grains which were consistent with the XRD results. Ferroelectricities of these specimens were confirmed by the measurement of polarization field hysteresis loops.

Keywords: $SrBi_2Ta_2O_9$ thin film; Crystallization; Lateral force microscopy; X-ray diffraction

1. Introduction

Strontium bismuth-tantalate ($SrBi_2Ta_2O_9$; SBT) thin films have been intensively studied for use as non-volatile ferroelectric random access memories (NVFRAM), as they have negligible polarization fatigue. Ferroelectric SBT thin films have the Bi-based layer-structure perovskite. The unit cell of SBT consists of stacking two perovskite-like units of $SrTaO_3$ between Bi_2O_3 layers, with a pseudotetragonal structure. Transmission electron microscopy (TEM) studies [1,2] of SBT thin films revealed that the first and second phase were identified involving circular grains > 200 nm and < 50 nm in diameter, respectively, and a third, amorphous phase occurs around these grains as a kind of matrix.

This paper presents the results of the atomic force microscopy and lateral force microscopy studies on the crystallization SBT films prepared onto platinized silicon wafers by the sol–gel method. The atomic force microscope (AFM) is a powerful tool for obtaining information of the three-dimensional surface morphology and the lateral force microscope (LFM), which is a modified version of the AFM, can be used for obtaining the friction coefficient from the measurement of the lateral forces acting between the probing tip and a flat sample. It is also possible to discriminate the different phases with different coefficients of friction distributed on the surface of samples by measuring both the three-dimensional surface morphology and the lateral force images scanned along both sides of an axis. In our experiment, both circular grains and matrix were observed in LFM images for specimens annealed below 675°C, which were consistent with the results of X-ray diffraction spectroscopy. The coefficients of friction of these two

* Corresponding author. Tel.: +82 371 7300310; fax: +82 371 7300308; e-mail: leekbae@unitel.co.kr

0040-6090/98/$ - see front matter
PII S0040-6090(98)01118-3

phases, i.e. SBT grain and matrix, were determined by comparing that of mica [3], and the ferroelectric properties of SBT films annealed above 700°C were also investigated.

2. Experiment

A few SBT films were synthesized by the metal-organic-decomposition spin-coating method with different post-annealing temperatures. Coating sol of SBT was prepared from appropriate proportion of bismuth 2-ethylhexanoate, strontium 2-ethyl hexanoate and tantalum ethoxide. The mole ratios of

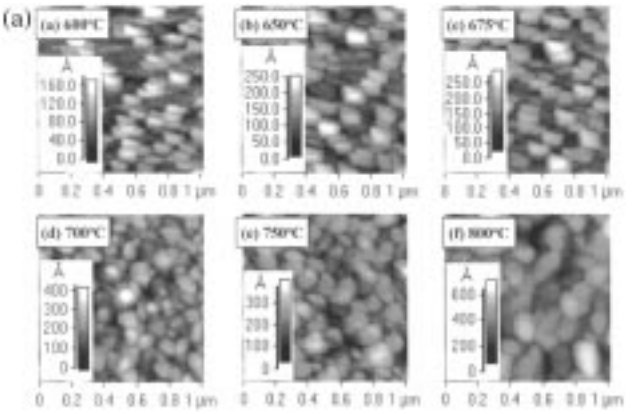

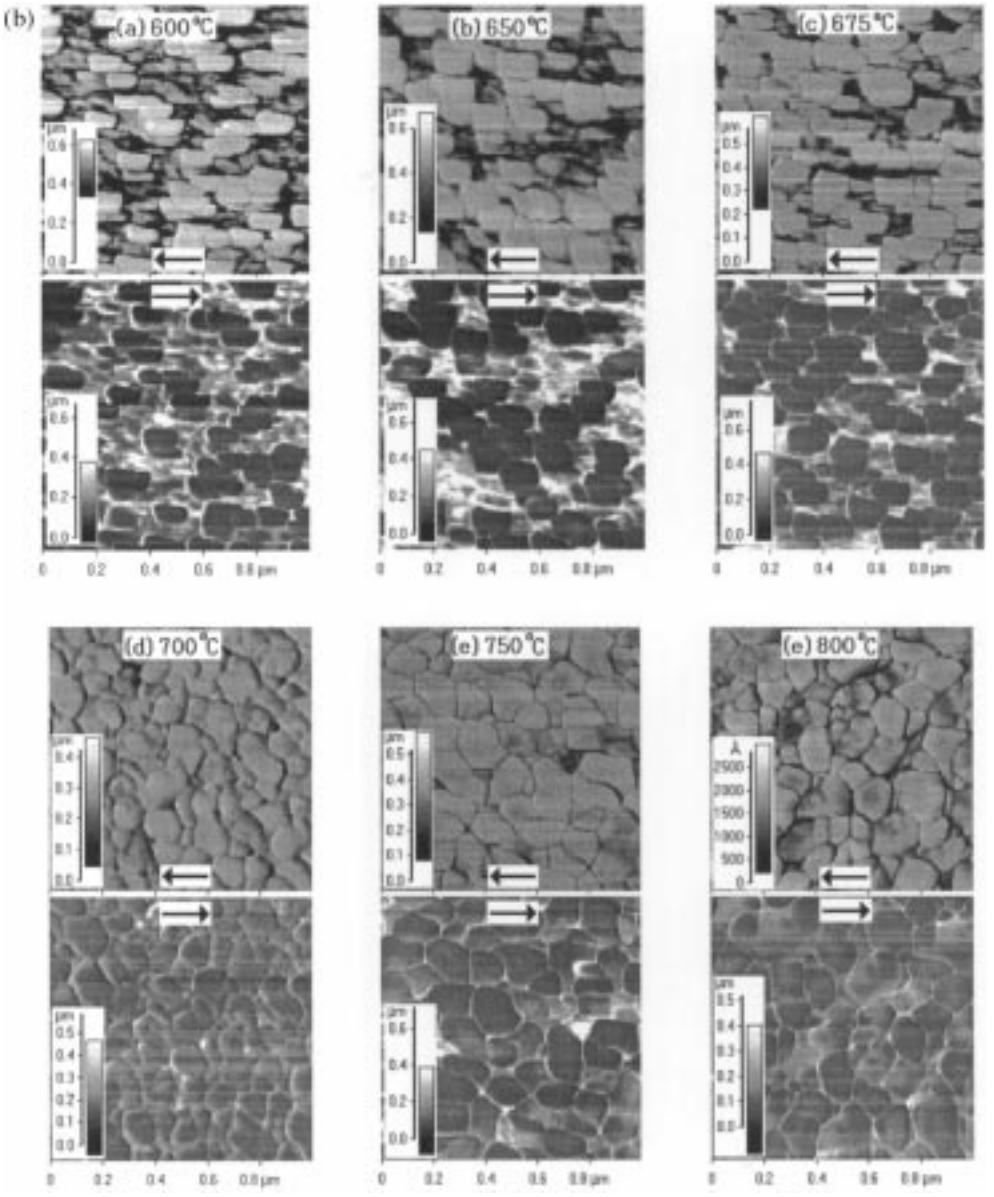

Fig. 1. The (a) AFM and (b) LFM images of the surface morphologies of $SrBi_2Ta_2O_9$ thin films annealed at different temperatures ranging from 600 to 800°C. Scanning direction in the LFM measurement is denoted as an arrow in Fig. 1b.

Sr/Ta and Bi/Ta in the SBT solution were 0.5 and 1.2, respectively. The solution was spin-casted onto platinized Si wafers at 3000 rev./min. The coated gel films were baked on a hot plate at 200°C for 1 min to evaporate the solvent and then heated at 600°C for 10 min in air to remove organic materials. After the process was repeated three times, the films were annealed at different temperatures ranging from 600 to 800°C for 10 min, respectively. The final thickness of SBT layer was approx. 280 nm.

To study the film surface, a scanning probe microscope (PSI Autoprobe AFM/LFM) with a commercial cantilever of force constant $k = 0.05$ N/m and a Si_3N_4 tip operated in contact mode was used. While the specimens were scanned perpendicular to the cantilever, the *z*-displacement and the torsion of the cantilever were measured by a four-segment photosensitive-position-detector. Hence, the data acquisitions were performed simultaneously in lateral force and constant force regime for frictional and topographic imaging, respectively. Such measurements were carried out in both directions of the *x*-axis, separately.

3. Results and discussions

Fig. 1 shows the typical AFM/LFM images of the surface of SBT films. An arrow on the top of the images in Fig. 1b denotes the scanning directions. It can be seen that in the AFM topographic images for all SBT films (Fig. 1a) grains and matrix are shown, which are nearly independent on the scanning direction. However, the LFM images (Fig. 1b), especially for specimens annealed below 675°C, are inverted in black and white by the scanning direction. These results indicate that two phases, i.e. grain and matrix, have different values of the coefficient of friction, attributed to the different compositions and microstructures. In the LFM images, it can also be seen that the value of the coefficient of friction for grains is smaller than that for the matrix as the larger sideways deflection by friction is brighter in LFM image for the scanning direction from left to right, and vice versa. The distribution ratio of grain which is defined as the ratio of the total area occupied by grains to the total area occupied by grains and the matrix is plotted as a function of annealing temperature in Fig. 2. As the annealing temperature increases, grains are more circular and the distribution ratio of grain increases up to 700°C before saturation. In Fig. 3, we present grain size and rms roughness obtained in the LFM and AFM topographic images, respectively, as a function of the annealing temperature. Grain size increases from 100 to 200 nm with an increase in annealing temperature. The rms roughness also increases with an increase in annealing temperature, which is believed to be due to the larger grain growth.

The coefficients of friction of grain and matrix were determined by acquiring the height profiles of the partial lines on the grain and the matrix denoted by (a) and (b) in the LFM images, as typically shown in Fig. 4. As the torsion constant of the cantilever used in our experiment was not known, the values of the coefficient of friction for grain and matrix, μ_{grain} and μ_{matrix}, were obtained by calibrating the LFM set-up by measuring the coefficient of friction of mica, μ_{mica}. Neglecting the adhesion force between the Si_3N_4-tip and the specimen due to the contamination layer, such as water, on both tip and specimen, μ_{grain} (or μ_{matrix}) is given as following;

$$\mu_{grain}(\text{or } \mu_{matrix}) = \mu_{mica} x_{grain}(\text{or } x_{matrix})/x_{mica} \quad (1)$$

where $\mu_{mica} = 0.071$ [3], and x is the sideways deflection of a tip along the *x*-axis by torsional force acting on a tip, which is determined as the average height of

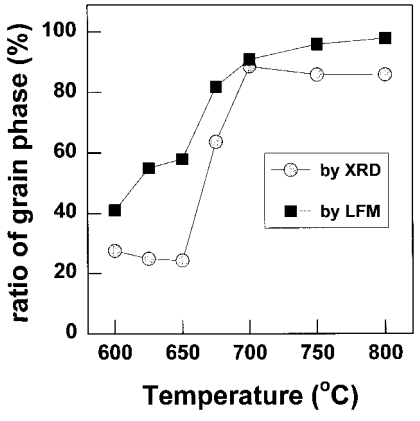

Fig. 2. Plot of the distribution ratio of grains obtained by LFM (squares) and XRD (circles) as a function of annealing temperature, where the distribution ratio of grains is defined as the ratio of the total area occupied by grains to the total area occupied by grains and matrix.

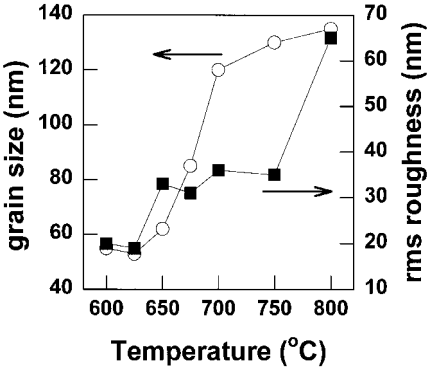

Fig. 3. Plot of grain size and rms roughness as a function of annealing temperature.

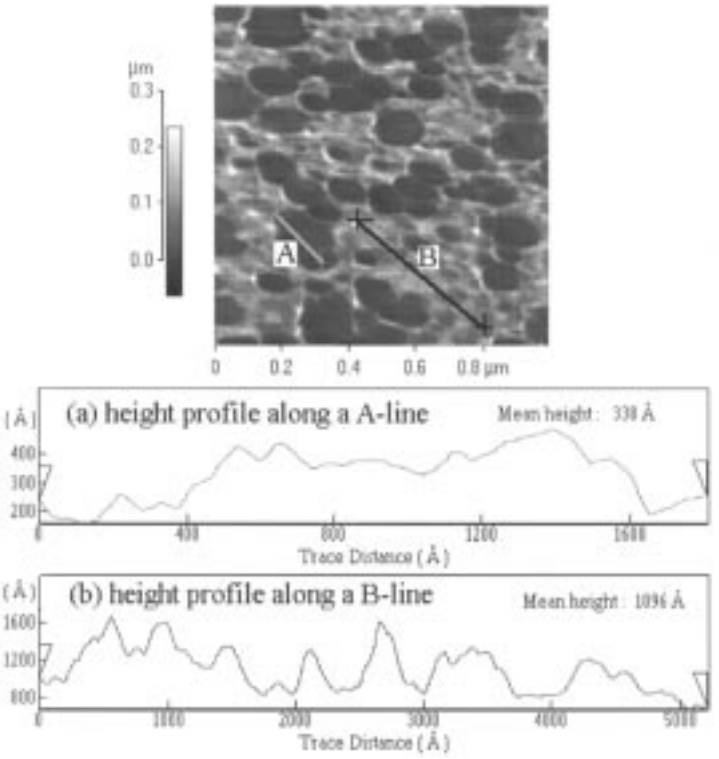

Fig. 4. Typical height profiles of two different phases: (a) grain; and (b) matrix, in LFM image of $SrBi_2Ta_2O_9$ thin film annealed at 600°C.

the frictional loop, as shown in Fig. 4. The measured values of μ_{grain} and μ_{matrix} for all specimens were 0.19 ± 0.08 and 0.28 ± 0.08, respectively.

To find the crystallinity of SBT films, XRD patterns were measured by means of the grazing incident method with the incident angle of 1.5°. Fig. 5 shows XRD patterns of SBT films fabricated at different annealing temperatures, and indicates that polycrystalline SBT films grown on Pt-coated Si wafer have no preferred orientation, especially for annealing temperatures above 675°C. The broad halos of amorphous phases appear around $2\theta = 28.5°$, 33.1° and 47.5° for SBT films annealed at 600–675°C, which are thought to correspond to the matrix phases in Fig. 1. Although, for specimens prepared at these ranges of annealing temperatures, XRD peaks corresponding to the Bi-layer perovskite SBT phases seem to be hidden by the overlapping broad halos, it is not hard to find their traces in XRD patterns. We tried to fit the XRD curves between $2\theta = 26°$ and 35° with four Gaussian functions having the maximum peak fixed at $2\theta =$ 29.05°, 32.45°, 28.05° and 33.15°, where the former two values correspond to the Bi-layered perovskite SBT (105) and (110) peaks, respectively, and the others correspond to the amorphous phases in SBT. One typical fitting of the XRD curve is shown in Fig. 6. The separate contributions of these two phases, i.e. SBT grains and matrix, can be calculated from their fitting parameters. When the Gaussian function has the form $y = A \exp[-B(x-C)^2]$, the area of the Gaussian, i.e. the integrated intensity, is given by: $A(\pi/B)^{1/2}$. We calculated the ratios of the integrated intensity of the perovskite SBT peaks to the total integrated intensity in the range of $2\theta = 26$–35° and then plotted them as a function of annealing temperature in Fig. 2, for comparison with the results obtained from the LFM measurement. It is very interesting that the behavior of the ratio of phases obtained by XRD with the annealing temperature is consistent with that by LFM. However, the LFM result is relatively larger than the XRD result in the

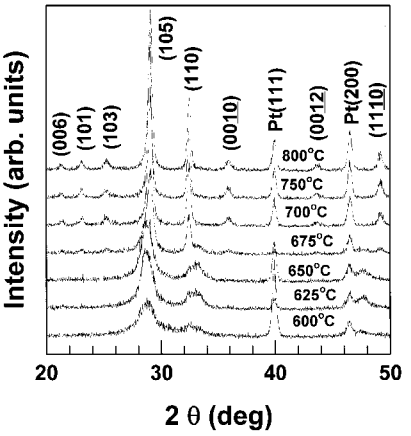

Fig. 5. Effect of annealing temperature on the XRD patterns of $SrBi_2Ta_2O_9$ thin films.

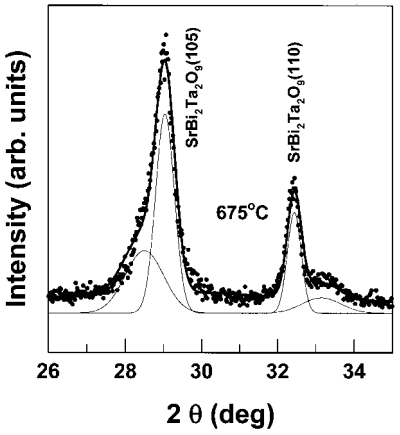

Fig. 6. Typical curve fitting of XRD pattern for $SrBi_2Ta_2O_9$ thin film. The measured XRD intensities are denoted by the symbol of filled circles and the thick-solid line is a fit with four Gaussian functions denoted as thin-solid lines.

low temperature regime, i.e. 600–650°C. We presume that such a result may be due to the following two possibilities. The first is that the apparent grains in the LFM images are not SBT polycrystalline grains but only boulders that have no Bi-layered perovskite phase. The second is that the volume distribution of SBT grains is different from the surface one, as the LFM result is attributed to the surface of the specimen while the XRD result is dominated by the volume. We suggest that the latter is more possible than the former. As the values of the frictional coefficients of grains are nearly constant in annealing temperature, grains in the LFM images are presumed not to be only boulders. In addition to the second possibility, we hypothesize that the crystallization by grain growth with increasing annealing temperature starts at the surface of SBT film and then progresses toward the Pt-bottom electrode. These crystallization processes in post-annealed growth used in the sol–gel method may be different from those in in situ growth of SBT film used in other methods such as liquid chemical vapor deposition [4], sputter deposition [5] and pulsed laser ablation deposition [6].

We determined some fundamental electrical properties of our SBT thin films. To measure the electrical properties of SBT thin films, a Pt-upper electrode with 0.3-mm diameter was sputtered on the SBT layer by r.f. magnetron sputtering using a shadow mask. The dielectric constant was measured using LCZ meter and P-E hysteresis curves were measured using a standard ferroelectric tester (Radiant Technologies, RT66A). Fig. 7 shows the dielectric constant values as a function of annealing temperature, which is nearly consistent with the results in Fig. 2. That is, the behavior of dielectric constant with annealing temperature is attributed to the phase ratio of perovskite SBT grains, even for specimens annealed below 675°C.

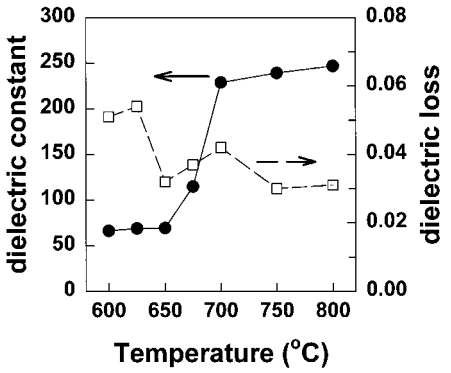

Fig. 7. Plot of dielectric constant and dielectric loss as a function of annealing temperature for $SrBi_2Ta_2O_9$ thin film.

Ferroelectricity of SBT thin films could be confirmed by the measurement of P-E hysteresis curves, as shown in Fig. 8. As expected in the XRD results, ferroelectricity was found for specimens annealed above 700°C. P-E hysteresis characteristics such as remnant polarization, P_r, and coercive field, E_c, are shown as a function of annealing temperature in the inset of Fig. 8. The behaviors of P_r and E_c with annealing temperature can also be interpreted in terms of the increase in the distribution ratio of SBT grains. The values of P_r and E_c for ferroelectric SBT film annealed at 800°C are 9.8 $\mu C/cm^2$ and 42 kV/cm, respectively.

4. Conclusion

We imaged crystalline grains and an amorphous matrix from AFM/LFM investigation of SBT surface. The distribution of these two phases was consistent with the results of the XRD measurements. The relationship between both dielectric constant and hysteresis characteristics and annealing temperature are attributed to the distribution of grains and matrix. Additionally, the relatively lower values of both di-

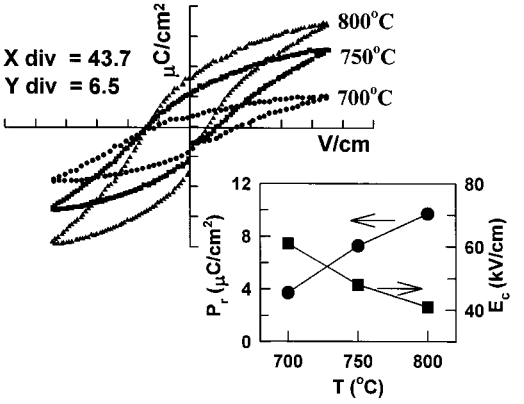

Fig. 8. P-E hysteresis loops of ferroelectric $SrBi_2Ta_2O_9$ thin films annealed above 700°C. The inset shows the plot of remnant polarization, P_r, and coercive field, E_c, vs. annealing temperature.

electric constant and remnant polarization for SBT film compared to the $Pb(Zr,Ti)O_3$ film, which is another promising NVFRAM material, are thought to be due to amorphous matrix existing around SBT grains even in ferroelectric SBT films.

References

[1] J.F. Scott, F.M. Ross, C.A. Paz de Araujo, M.C. Scott, M. Huffman, MRS Bull. 27 (1996) 33.

[2] I. Koiwa, T. Kanehara, J. Mita, et al., Jpn. J. Appl. Phys. 35 (1996) 4946.

[3] C. Putman, M. Igarashi, R. Kaneko, Jpn. J. Appl. Phys. 34 (1995) L264.

[4] L.D. McMillan, C.A. Paz de Araujo, T. Roberts, J.J. Cuchiaro, M.C. Scott, J.F. Scott, Ferroelectrics 2 (1992) 351.

[5] K. Amanuma, T. Hase, Y. Miyasaka, Appl. Phys. Lett. 66 (1994) 221.

[6] R. Dat, J.K. Lee, O. Auciello, A.I. Kinggon, Appl. Phys. Lett. 67 (1995) 572.